

# Amyloids protect the silkmoth oocyte and embryo

Vassiliki A. Iconomidou<sup>a</sup>, Gert Vriend<sup>b</sup>, Stavros J. Hamodrakas<sup>a,\*</sup>

<sup>a</sup>Department of Cell Biology and Biophysics, Faculty of Biology, University of Athens, Panepistimiopolis, Athens 157 01, Greece  
<sup>b</sup>European Molecular Biology Laboratory, Meyerhofstrasse 1, Postfach 10.2209, 69012 Heidelberg, Germany

Received 20 June 2000; revised 16 July 2000; accepted 23 July 2000

Edited by Gunnar von Heijne

**Abstract** Chorion is the major component of silkmoth eggshell. More than 95% of its dry mass consists of proteins that have remarkable mechanical and chemical properties protecting the oocyte and the developing embryo from a wide range of environmental hazards. We present data from electron microscopy (negative staining and shadowing), X-ray diffraction and modeling studies of synthetic peptide analogues of silkmoth chorion proteins indicating that chorion is a natural amyloid. The folding and self-assembly models of chorion peptides strongly support the  $\beta$ -sheet helix model of amyloid fibrils proposed recently by Blake and Serpell [Structure 4 (1996) 989–998]. © 2000 Federation of European Biochemical Societies. Published by Elsevier Science B.V. All rights reserved.

**Key words:** Silkmoth chorion protein; Amyloid fibril; Electron microscopy; X-ray diffraction; Modeling

## 1. Introduction

The major component of the eggshell of many insect and fish eggs is chorion. Proteins account for more than 95% of its dry mass. This proteinaceous shell forms an outer layer of the eggshell and has extraordinary mechanical and physiological properties, protecting the oocyte and the developing embryo from a series of environmental hazards such as temperature variations, mechanical pressure, proteases, bacteria, viruses, etc. [1]. Fig. 1a shows an electron micrograph of a thin transverse section of a silkmoth chorion. A lamellar ultrastructure of packed fibrils is seen: silkmoth chorion is a biological analogue of a cholesteric liquid crystal [2,3]. The X-ray diffraction pattern of a silkmoth chorion shown in Fig. 1b indicates that  $\beta$ -sheet is the dominant secondary structure of its constituent proteins. Fourier transform infrared (FT-IR) [3], laser Raman spectroscopy [4,5] and X-ray diffraction studies [6,7] suggest that the  $\beta$ -sheets are antiparallel.

About 200 proteins have been detected in the silkmoth chorion [8]. These proteins have been classified into two major classes, A and B [1]. The gene families encoding these proteins are related and constitute a superfamily with two branches, the  $\alpha$ -branch and the  $\beta$ -branch [9]. Sequence analyses and secondary structure prediction revealed that chorion proteins consist of three domains [10]. The central domain is conserved in each of the two classes. The flanking N- and C-terminal domains are more variable and contain characteristic tandem repeats ([10]; see also Fig. 2). A and B central domains show

distant similarities suggesting that the chorion genes constitute a superfamily derived from a single ancestral gene [9].

The study of the properties of chorion proteins has long been hampered by the fact that it has proven very difficult to purify individual chorion proteins in large enough amounts of sufficient purity for structural studies. We therefore synthesized a 51-residue peptide [11] that can be considered a generic

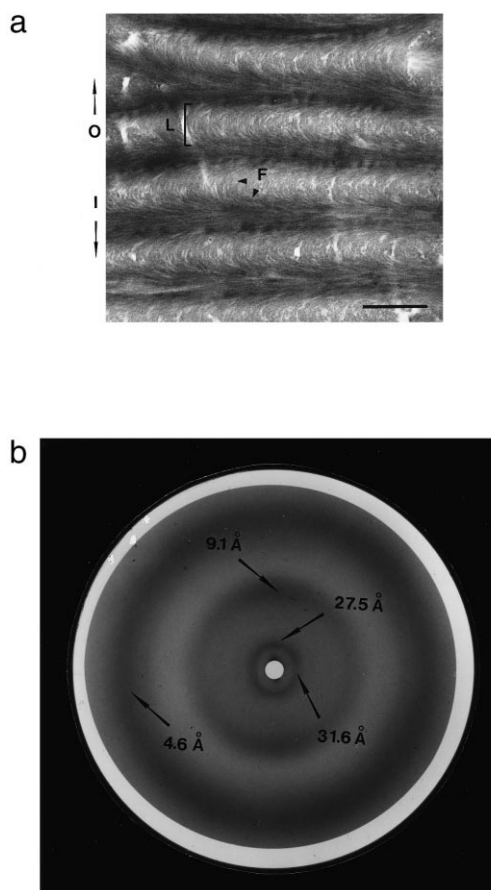


Fig. 1. a: Transmission electron micrograph of an oblique section through the helicoid proteinaceous chorion of the silkmoth *A. polyphemus*. Arrays of protein fibrils (ca. 100 Å, F, arrowheads) are seen in each lamella (L). Arrows point towards the outer (O) and inner (I), closest to the oocyte, surfaces of chorion. Bar: 0.4  $\mu$ m. b: X-ray diffraction pattern from an almost flat fragment of a silkmoth *A. polyphemus* chorion. The flat fragment of chorion was irradiated with the X-ray beam parallel to the outer and inner surfaces of chorion (panel a corresponds to a cut face of chorion that would be encountered by the beam). The presence of reflections corresponding to periodicities of 4.6 and 9.1 Å suggests abundance of  $\beta$ -sheet in chorion proteins. The elliptical scattering at ca.  $30 \text{ \AA}^{-1}$  indicates a helicoid architecture for silkmoth chorion and most probably arises from ca. 30 Å protofilaments, constituents of the ca. 100 Å fibrils [3].

\*Corresponding author. Fax: (30)-1-7231634.  
E-mail: shamodr@cc.uoa.gr

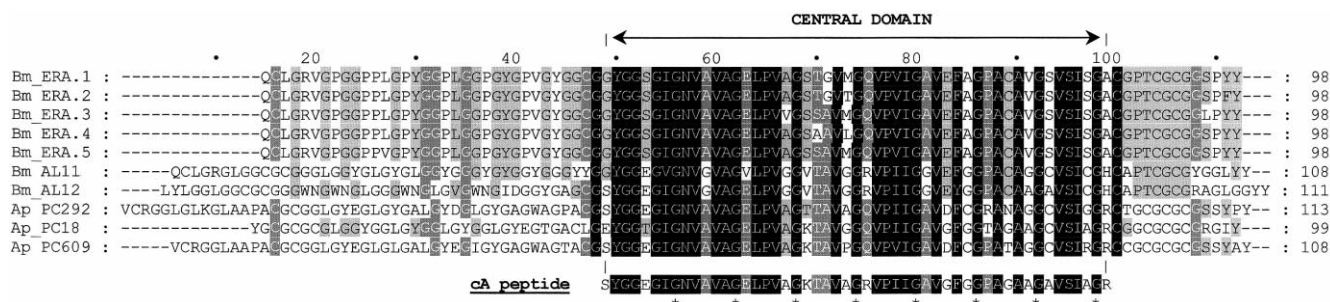


Fig. 2. Alignment of several chorion proteins of the A class ([3] and references therein). The names of the proteins are to the left of each sequence. The designations Bm and Ap refer to *Bombyx mori* and *A. polyphemus* respectively. By convention 'pc' numbers refer to sequences derived from cDNA clones, whereas the initials ERA and AL refer to 'early' A and 'late' A proteins respectively. Numbers to the right of each sequence are the total number of residues of each protein. The borders of the central conservative domain are marked at the top (by arrows). The numbering at the top is arbitrary. Black-boxed residues are identical and gray-boxed residues represent conservative substitutions. Alignments were created with CLUSTALX [32] and shading was done with GeneDoc 2.5.0 (Windows 95 version) [33]. The cA peptide sequence is shown at the bottom. Asterisks at the bottom mark invariant Gly (G) residues.

central domain of the A class of silkworm chorion proteins (Fig. 2). This peptide, referred to below as cA peptide, is representative for about 30% of all the proteinaceous material in the eggshell. We chose this peptide because the central domains of the A class chorion proteins are highly conserved in both sequence and length and because this conservation indicates that this domain plays an important functional role in the formation of chorion structure. Laser Raman and FT-IR experiments showed that the structure of the cA peptide is predominantly antiparallel  $\beta$ -pleated sheet both in solution and in the solid state [11].

## 2. Materials and methods

### 2.1. X-ray diffraction

cA peptide was dissolved in a 50 mM sodium acetate buffer (pH 5) at a concentration of 9 mg/ml to produce amyloid-like fibrils after 3–4 weeks incubation. A droplet ( $\sim 10 \mu\text{l}$ ) of fibril suspension was placed between two siliconized glass rods, spaced  $\sim 2$  mm apart and mounted horizontally, as colinearly as possible. It was allowed to dry at ambient temperature and humidity for 1 h to form an oriented fiber suitable for X-ray diffraction. X-ray patterns were obtained immediately from these fibers since it was found that fiber orientation was lost after  $\sim 2$  h under these conditions. X-ray diffraction patterns were recorded on a Mar Research 345mm image plate, utilizing double-mirror (Prophysics mirror system XRM-216) focused  $\text{CuK}\alpha$  radiation ( $\lambda = 1.5418 \text{ \AA}$ ), obtained from a GX-21 rotating anode generator (Elliot-Marconi Avionics, Hertfordshire, UK) operated at 40 kV, 75 mA. The specimen-to-film distance was set at 150 mm and the exposure time was 1 h. No additional low angle reflections were observed at longer specimen-to-film distances of up to 300 mm. The X-ray patterns, initially viewed using the program MarView (Mar Research, Hamburg, Germany), were displayed and measured with the aid of the program IPDISP of the CCP4 package [12].

### 2.2. Negative staining

For negative staining, cA peptide fibril suspensions (as above) were applied to glow-discharged 400 mesh carbon-coated copper grids for 60 s. The grids were (occasionally) flash-washed with  $\sim 150 \mu\text{l}$  of buffer and stained with a drop of 1% (w/v) aqueous uranyl acetate for 45 s. Excess stain was removed by blotting with a filter paper and the grids were air-dried. They were examined in Philips 400T or CM120 transmission electron microscopes operated at 100 kV.

### 2.3. Rotary shadowing

Samples were deposited onto carbon-coated grids (400 mesh), flash-washed with buffer and left to dry in air after blotting the liquid excess with a filter paper. Dried grids were mounted on a rotating table in an Edwards vacuum evaporator and coated with a thin layer of platinum/palladium at a shadowing angle of  $7^\circ$ , under high vac-

uum. Rotary-shadowed grids were observed in Philips 400T or CM120 electron microscopes, operated at 100 kV.

### 2.4. Modeling

The antiparallel  $\beta$ -pleated sheet model (Fig. 4b) was built by extracting from the PDB [13]  $\beta$ -hairpins with sequences that resembled the cA peptide sequence motifs as closely as possible. These  $\beta$ -hairpins were extracted with enough length to provide overlap, and this overlap was used to superpose subsequent hairpins. The final model was converted by homology modeling into the cA peptide antiparallel  $\beta$ -pleated sheet model, utilizing the WHAT IF [14] program. The model was regularized with the WHAT IF regularization options [14]. The left-handed  $\beta$ -helix model of the cA peptide (Fig. 4d) was produced by homology modeling, using the UDP-*N*-acetylglucosamine acyltransferase structure [15] as a template in conjunction with the WHAT IF [14] program. The model was optimized employing the GROMOS molecular dynamics software [16]. The MOLSCRIPT [17] program was used to produce ribbon diagrams of the models.

## 3. Results and discussion

The cA peptide forms structurally uniform, amyloid-like fibrils by self-assembly in various solvents, pH values, ionic strengths and temperatures (V.A. Iconomidou and S.J. Hamodrakas, in preparation). The fibrils were judged to be amyloid-like from their tinctorial and structural characteristics: they bind Congo red showing the red-green birefringence characteristic for amyloids when seen under crossed polars ([18] and references therein) as well as thioflavine-T (data not shown). Electron micrographs (Fig. 3a,b) show that they are straight, unbranched double helices of indeterminate length and uniform in diameter ( $\sim 90 \text{ \AA}$ ). Each double-helical fibril consists of two protofilaments wound around each other. The protofilaments both have a uniform diameter of approximately 30–40  $\text{ \AA}$ . The pitch of the double helix (Fig. 3a, arrows) is approximately 920  $\text{ \AA}$ .

Suspensions of these fibrils form oriented fibers, which give characteristic 'cross- $\beta$ ' X-ray diffraction patterns (Fig. 3c). In these oriented fibers, the long axes of the amyloid-like fibrils seen in the electron micrographs of Fig. 3a,b are oriented more or less parallel to the fiber axis [19].

The oriented X-ray pattern (Fig. 3c) taken from these fibers indicates the presence of oriented  $\beta$ -sheets in the amyloid-like fibrils of peptide cA. The presence of reflections corresponding to periodicities of 4.66 and 10.12  $\text{ \AA}$  indicates the existence of  $\beta$ -sheets. The strong meridional reflection at 4.66  $\text{ \AA}$  sug-

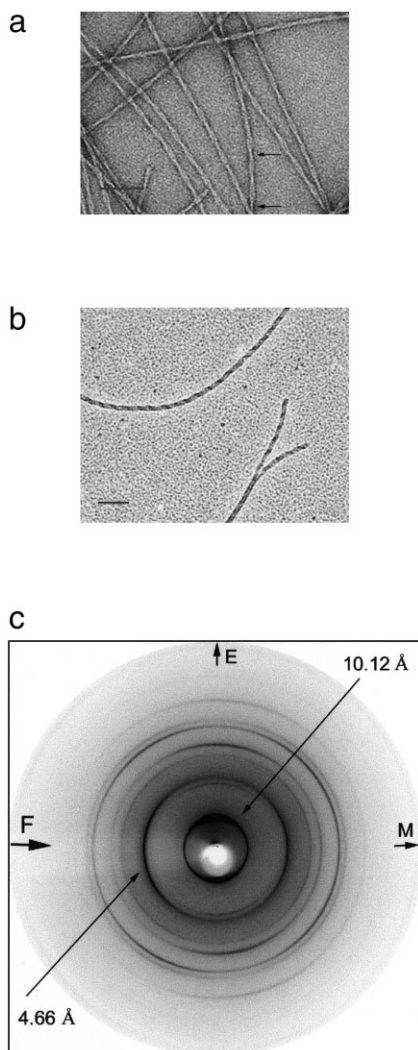


Fig. 3. a: Electron micrograph of amyloid-like fibrils derived by self-assembly, from a 9 mg/ml solution of the cA peptide in a sodium acetate 50 mM buffer, pH 5. Fibrils are negatively stained with 1% uranyl acetate. They are of indeterminate length (several micrometers), unbranched, approximately 90 Å in diameter and have a double-helical structure. The pitch of the double helix is  $\sim 920$  Å (marked with arrows). A pair of protofilaments each 30–40 Å in diameter are wound around each other, forming the double-helical fibrils. Bar: 800 Å. b: Electron micrograph of amyloid-like fibrils derived from a solution of the cA peptide (conditions as in panel a). Fibrils are rotary shadowed with Pt/Pd at an angle of  $7^\circ$  under high vacuum. Bar: 1000 Å. c: X-ray diffraction pattern from an oriented fiber of cA peptide amyloid-like fibrils. The meridian, M (direction parallel to the fiber axis), is horizontal and the equator, E, is vertical in this display. The X-ray diffraction pattern is a typical ‘cross- $\beta$ ’ pattern showing a 4.66 Å reflection on the meridian and a 10.12 Å reflection on the equator. This indicates a regular structural repeat of 4.66 Å along the fiber axis (meridian) and a structural spacing of 10.12 Å perpendicular to the fiber axis. The structural repeat of 4.66 Å along the fiber axis corresponds to the spacing of adjacent  $\beta$ -strands (which should be perpendicular to the fiber axis, a ‘cross- $\beta$ ’ structure) and the 10.12 Å spacing perpendicular to the fiber axis corresponds to the face-to-face separation (packing distance) of the  $\beta$ -sheets.

gests that the  $\beta$ -sheets are oriented so that their  $\beta$ -strands are perpendicular to the fiber axis and thus also to the long axis of the amyloid-like fibrils. The strong equatorial reflection at 10.12 Å, which corresponds to the inter-sheet distance, suggests that the packing of the  $\beta$ -sheets is parallel to the fiber

axis and preferentially oriented. This X-ray pattern closely resembles typical cross- $\beta$  patterns taken from amyloid fibers ([18] and references therein).

A list of the meridional and equatorial reflections observed in the X-ray pattern (Fig. 3c) is given in Table 1. Reflections along the meridian are orders of the 115 Å spacing ( $116 \pm 1$  Å) of the  $\beta$ -helix of the amyloid protofilament model proposed by Blake and Serpell [25], which supports this model. Reflections along the equator are orders of the 10.12 Å inter-sheet distance indicating a long range order of packed  $\beta$ -sheets in the fiber.

The model for the structure of the cA peptide that accounts for all our data, as well as for all data gathered previously [3,20,21], is shown in Fig. 4a,b. The structural fold of cA is most probably an antiparallel twisted  $\beta$ -pleated sheet of four-residue  $\beta$ -strands alternating with type II'  $\beta$ -turns. Invariant Gly residues occupy the second position of the  $\beta$ -turns, a location especially favorable for Gly in II' turns of twisted  $\beta$ -sheets of globular proteins [22].

Another interesting possibility for the structure of the cA peptide might be that of the left-handed parallel  $\beta$ -helix found in the structure of UDP-*N*-acetylglucosamine acyltransferase [15]. This protein shows hexapeptide sequence motifs. It is interesting to note that right-handed parallel  $\beta$ -helices similar to those found in the pectate lyases have been postulated as the main molecular components of amyloid protofibrils [23]. Characteristic hexapeptide periodicities of both Gly and hydrophobic residues also appear in the sequence of the cA peptide [3]. Its sequence shows structural similarities with the sequence of UDP-*N*-acetylglucosamine acyltransferase (Fig. 4c), and the peptide would have a nice hydrophobic core when folded this way (Fig. 4d).

However, preliminary calculations of X-ray diffraction patterns from the models presented in Fig. 4b,d and comparison with the experimental diffraction pattern of Fig. 3c, as well as analysis of the amide I band of FT Raman and FT-IR spectra taken from samples containing amyloid-like fibrils formed from the cA peptide (V.A. Ionomidou and S.J. Hamodrakas, in preparation) support the antiparallel twisted  $\beta$ -pleated sheet model shown in Fig. 4b.

Twenty-five years ago, it was suggested that, because of the inherent twist of the  $\beta$ -sheets in the monomer, the polymeric amyloid protofilaments might form long spacing helical structures in which the protofilaments are intertwined to produce 100 Å doubly helical amyloid fibrils [24]. The verbal description of this model, reminiscent of the  $\beta$ -helix structure of

Table 1  
Spacings of the meridional and equatorial reflections, observed in the X-ray diffraction pattern taken from an oriented fiber of cA peptide amyloid-like fibrils (Fig. 3c)

Meridian		Equator	
$d_{\text{obs}}$ (Å)	Index	$d_{\text{obs}}$ (Å)	Index
4.66	25	10.12	
3.63	32	5.05	2
2.92	40	3.33	3
2.81	41	2.52	4
2.27	51		
2.12	55		

Indexing was done assuming a repeat period of  $116 \pm 1$  Å for the meridional reflections. The equatorial reflections are orders of the 10.12 Å inter-sheet packing distance.

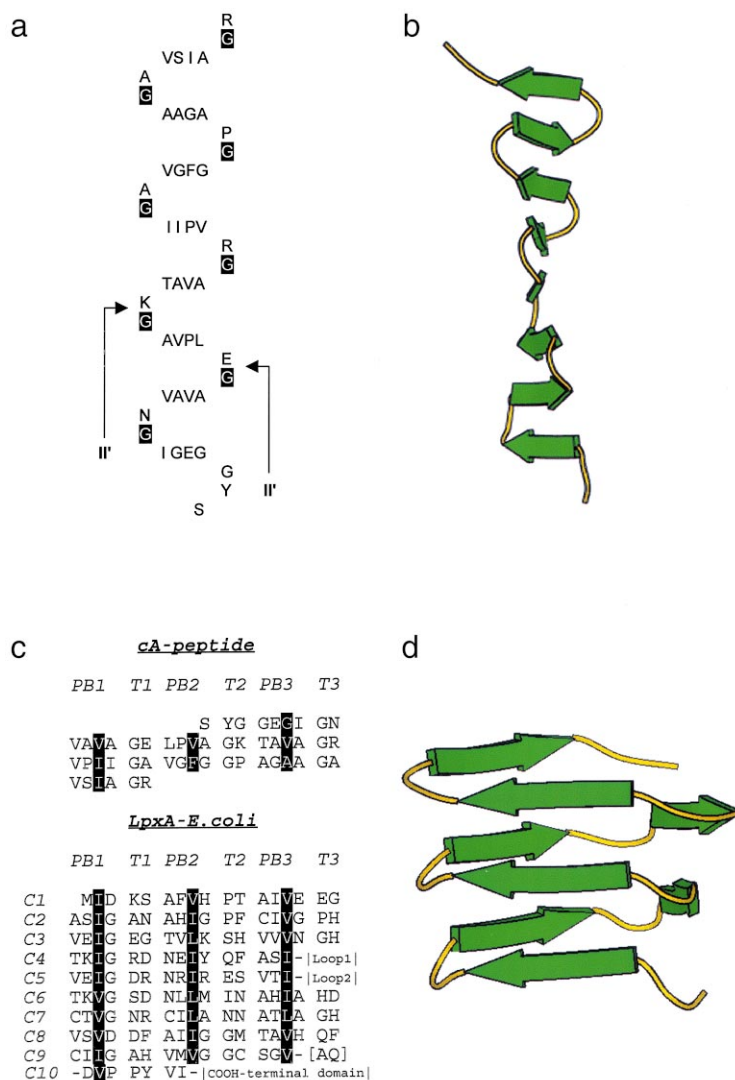


Fig. 4. a: Antiparallel twisted  $\beta$ -sheet model proposed for the cA peptide. Sequence should be read continuously, beginning at the bottom. Invariant glycines (G) occupying the second position in the  $\beta$ -turns are black-boxed. Tentative II'  $\beta$ -turns alternate with four-residue  $\beta$ -strands. b: A ribbon representation [17] of the antiparallel twisted  $\beta$ -sheet model proposed for the cA peptide. View approximately along the central  $\beta$ -strands denoted as arrows. c: Structurally based alignment of the sequence of the cA peptide with the sequence of the N-terminal domain of UDP-N-acetylglucosamine acyltransferase (LpxA-*Escherichia coli*) [15]. The one-letter code is used. Sequences should be read continuously beginning at the top. The structure of the N-terminal domain of LpxA-*E. coli* is a left-handed parallel  $\beta$ -helix [15]. Rows C1 to C10 identify individual turns of the helix. PB1, PB2 and PB3 denote the parallel  $\beta$ -strands of each turn. T1, T2 and T3 denote turn residues. Conserved hydrophobic residues which have their side chains pointing towards the interior of the left-handed parallel  $\beta$ -helix to form the hydrophobic core, are black boxed. d: A ribbon representation [17] of the cA peptide in a left-handed parallel  $\beta$ -helix conformation (see Section 2). Arrows denote  $\beta$ -strands. View almost perpendicular to a face of the left-handed parallel  $\beta$ -helix.

transferrin amyloid protofilament produced 20 years later by high-resolution X-ray studies [25], fits well with our data. We postulate that successive cA units form continuous twisted antiparallel  $\beta$ -sheets (the so-called  $\beta$ -sheet helices following the nomenclature proposed by Blake and Serpell [25]) along the protofilaments of Fig. 3a, with their  $\beta$ -strands perpendicular to the long axis of the protofilaments ('cross- $\beta$ ' structures). The thickness of each individual cA unit is of the order of 30–40 Å, similar to the thickness of the individual protofilaments. Suspiciously, the pitch of the double-helical amyloid fibril formed by the two intertwined protofilaments is 920 Å (Fig. 3a), a multiple of the 115 Å spacing of the  $\beta$ -helix in the transthyretin amyloid protofilament [25]. Furthermore, the antiparallel twisted  $\beta$ -pleated sheet model of the cA peptide is an eight-stranded antiparallel  $\beta$ -sheet (Fig. 4a,b), in contrast

to the six-stranded  $\beta$ -sheet of transthyretin. According to Sunde and Blake [26], an eight-stranded  $\beta$ -sheet could well form a ' $\beta$ -sheet helix' instead of a six-stranded  $\beta$ -sheet.

We have shown that cA peptide fibrils have an amyloid nature, but we have so far silently assumed that the peptide fibrils are truly representative of the structure of chorion proteins in the eggshell. The cA peptide corresponds to about 30% of the total chorion mass. Its self-assembly mechanisms produce amyloid-like fibrils under a great and diverse variety of conditions (V.A. Iconomidou and S.J. Hamodrakas, in preparation), which strongly suggests that it should fold in an amyloid fashion also in the physiological state. Concomitant evidence for this assumption can be found in Fig. 1a. Lamellae (layers) of fibrils with the same dimensions (70–100 Å; see also [1,2]) as the cA peptide double-helical fibrils

shown in Fig. 3a constitute the helicoid architecture of silkmoth chorion. Chorion fibrils consist of 30–40 Å protofilaments with a helical structure [3,7]. Furthermore, antiparallel  $\beta$ -pleated sheet is the dominant molecular conformation of silkmoth chorion proteins in vivo ([3] and references therein).

Amyloids are generally associated with diseases such as Alzheimer's, spongiform encephalopathies, type II diabetes, etc.: at least 16 types of human disease are associated with the deposition of protein fibrils forming amyloids and resulting in tissue damage and degeneration [27,28]. Amyloidogenic proteins appear to be related by their ability to undergo a conformational change and adopt a new amyloidogenic conformation under partially denaturing conditions in vivo, which permits self-assembly into amyloid [28,29]. Our study shows that not all amyloids are by definition harmful. In chorion protein amyloids, the amyloidogenic conformation is, apparently, the native conformation. We believe that chorion proteins and peptide analogues provide a model system for the study of amyloid formation, and perhaps we can even extract medically relevant information from the chorion destruction mechanisms [30] used by the embryo upon hatching.

To our knowledge, this is the first well documented case where amyloid-like fibrils are formed from a peptide which has a sequence so clearly folded in an antiparallel  $\beta$ -pleated sheet type of structure of the 'cross- $\beta$ ' type. Nature, after millions of years of molecular evolution, has designed these amyloid-like chorion peptides to play an important functional role: to protect the oocyte and the developing embryo from a wide range of environmental hazards [1,3]. Chorion proteins self-assemble extracellularly to form the chorion of silkmoths, far away from the follicle cells that synthesize and secrete them [3]. It may be argued that this is not the only case where amyloids appear in vivo. The *Chrysopa flava* silk [31] might be another such paradigm.

**Acknowledgements:** V.A.I. gratefully acknowledges the help of a short-term EMBO fellowship. We thank Dr. L. Serrano, Dr. P. Tucker, Mr. P. Everitt, Dr. B. Agianian, Dr. K. Leonard and Dr. A. Hoenger for their help with the experiments. Special thanks are due to Prof. F.C. Kafatos for his unfailing interest and help. S.J.H. thanks the Greek Ministry of Research and Technology for financial support and the EMBL summer visitors program.

## References

- [1] Kafatos, F.C., Regier, J.C., Mazur, G.D., Nadel, M.R., Blau, H.M., Petri, W.H., Wyman, A.R., Gelinis, R.E., Moore, P.B., Paul, M., Efstratiadis, A., Vournakis, J.N., Goldsmith, M.R., Hunsley, J.R., Baker, B., Nardi, J. and Koehler, M. in: Results and Problems in Cell Differentiation (W. Beerman, Ed.), Vol. 8, pp. 45–145, Springer-Verlag, Berlin.
- [2] Mazur, G.D., Regier, J.C. and Kafatos F.C. (1982) in: Insect Ultrastructure (Akai, H. and King R.C., Eds.), Vol. 1, pp. 150–183, Plenum Press, New York.
- [3] Hamodrakas, S.J. (1992) in: Results and Problems in Cell Differentiation (Case, S.T., Ed.), Vol. 19 (Ch. 6), pp. 115–186, Springer-Verlag, Berlin.
- [4] Hamodrakas, S.J., Asher, S.A., Mazur, G.D., Regier, J.C. and Kafatos, F.C. (1982) *Biochim. Biophys. Acta* 703, 216–222.
- [5] Hamodrakas, S.J., Kamitsos, E.I. and Papanicolaou, A. (1984) *Int. J. Biol. Macromol.* 6, 333–336.
- [6] Hamodrakas, S.J., Paulson, J.R., Rodakis, G.C. and Kafatos, F.C. (1983) *Int. J. Biol. Macromol.* 5, 149–153.
- [7] Hamodrakas, S.J., Margaritis, L.H., Papisideri, I. and Fowler, A. (1986) *Int. J. Biol. Macromol.* 8, 237–242.
- [8] Regier, J.C. and Kafatos, F.C. (1985) in: *Comprehensive Insect Biochemistry, Physiology and Pharmacology* (Gilbert, L.I. and Kerkut, G.A., Eds.), Vol. 1, pp. 113–151, Pergamon Press, Oxford.
- [9] Lekanidou, R., Rodakis, G.C., Eickbush, T.H. and Kafatos, F.C. (1986) *Proc. Natl. Acad. Sci. USA* 83, 6514–6518.
- [10] Hamodrakas, S.J., Jones, C.W. and Kafatos, F.C. (1982) *Biochim. Biophys. Acta* 700, 42–51.
- [11] Benaki, D.C., Aggeli, A., Chryssikos, G.D., Yiannopoulos, Y.D., Kamitsos, E.I., Brumley, E., Case, S.T., Boden, N. and Hamodrakas, S.J. (1998) *Int. J. Biol. Macromol.* 23, 49–59.
- [12] Collaborative Computational Project, Number 4, The CCP4 Suite: Programs for Protein Crystallography (1994) *Acta Crystallogr. D50*, 760–763.
- [13] Berman, H.M., Westbrook, J., Feng, Z., Gilliland, G., Bhat, T.N., Weissig, H., Shindyalov, I.N. and Bourne, P.E. (2000) *Nucleic Acids Res.* 28, 235–242.
- [14] Vriend, G. (1990) *J. Mol. Graph.* 8, 52–56.
- [15] Raetz, C.R.H. and Roderick, S.R. (1995) *Science* 270, 997–1000.
- [16] Van Gunsteren, W.F. and Berendsen, H.J. (1987) *BIOMOS*, Biomolecular software. Lab. Phys. Chem., Univ. Groningen, The Netherlands.
- [17] Kraulis, P.J. (1991) *J. Appl. Crystallogr.* 24, 946–950.
- [18] Sunde, M. and Blake, C. (1997) *Adv. Protein Chem.* 50, 123–159.
- [19] Fraser, R.D.B. and MacRae T.P. (1973) *Conformation in Fibrous Proteins and Related Synthetic Polypeptides*, Academic Press, New York.
- [20] Hamodrakas, S.J., Etmektzoglou, T. and Kafatos, F.C. (1985) *J. Mol. Biol.* 186, 583–589.
- [21] Hamodrakas, S.J., Bosshard, H.E. and Carlson, C.N. (1988) *Protein Eng.* 2, 201–207.
- [22] Sibanda, B.L. and Thornton, J.M. (1985) *Nature* 316, 170–174.
- [23] Lazo, N.D. and Downing, D.T. (1998) *Biochemistry* 37 (7), 1731–1735.
- [24] Cooper, J.H. (1976) in: *Amyloidosis* (Wegelius, O. and Pasternak, A., Eds.), pp. 61–68, Academic Press, London.
- [25] Blake, C.C.F. and Serpell, L.C. (1996) *Structure* 4, 989–998.
- [26] Sunde, M. and Blake, C. (1998) *Q. Rev. Biophys.* 31, 1–39.
- [27] Pepys, M.B. (1996) in: *The Oxford Textbook of Medicine*, 3rd edn. (Weatherall, D.J., Ledingham, J.G.G. and Warrell, D.A., Eds.), Vol. 2, pp. 1512–1524, Oxford University Press, Oxford.
- [28] Kelly, J.F. (1996) *Curr. Opin. Struct. Biol.* 6, 11–17.
- [29] Kelly, J.F. (1998) *Curr. Opin. Struct. Biol.* 8, 101–106.
- [30] Hagenmaier, H.E. (1974) *Comp. Biochem. Physiol.* 49b, 313–324.
- [31] Geddes, A.J., Parker, K.D., Atkins, E.D.T. and Beighton, E. (1968) *J. Mol. Biol.* 32, 343–358.
- [32] Thompson, J.D., Gibson, T.J., Plewniak, F., Jeanmougin, F. and Higgins, D.G. (1997) *Nucleic Acids Res.* 24, 4876–4882.
- [33] Nicholas, K.B., Nicholas Jr., H.B. and Deerfield, D.W. (1997) *EMBNEW.NEWS* 4, 14.